Supplemental Data

American Journal of Human Genetics, Volume *88*

The Essential Role of Centrosomal NDE1 in Human Cerebral Cortex Neurogenesis

Mehmet Bakircioglu, Ofélia P Carvalho, Maryam Khurshid, James J Cox, Beyhan Tuysuz, Tanyeri Barak, Saliha Yilmaz, Okay Caglayan, Alp Dincer, Adeline K Nicholas, Oliver Quarrell, Kelly Springell, Gulshan Karbani, Saghira Malik, Caroline Gannon, Eamonn Sheridan, Moira Crosier, Steve N Lisgo, Susan Lindsay, Kaya Bilguvar, Fanni Gergely, Murat Gunel, C Geoffrey Woods

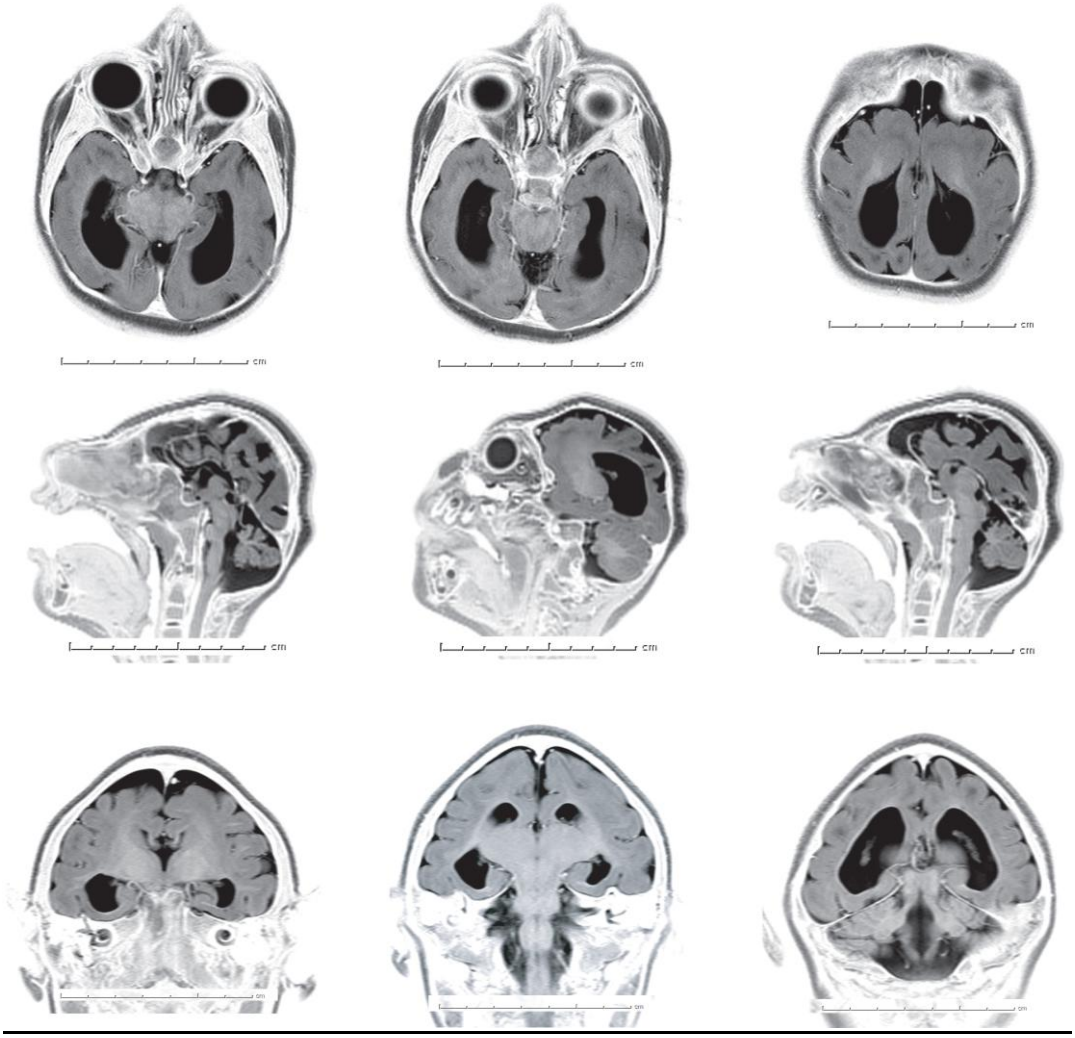

Figure S1. Detailed Brain Scans

MR image series of an affected child (Family C individual V-1). Axial, sagittal, and coronal MR images show severe microcephaly with cortical simplification, agenesis of corpus callosum and hypoplastic cerebellum. Photographically inverted T2 images are shown.

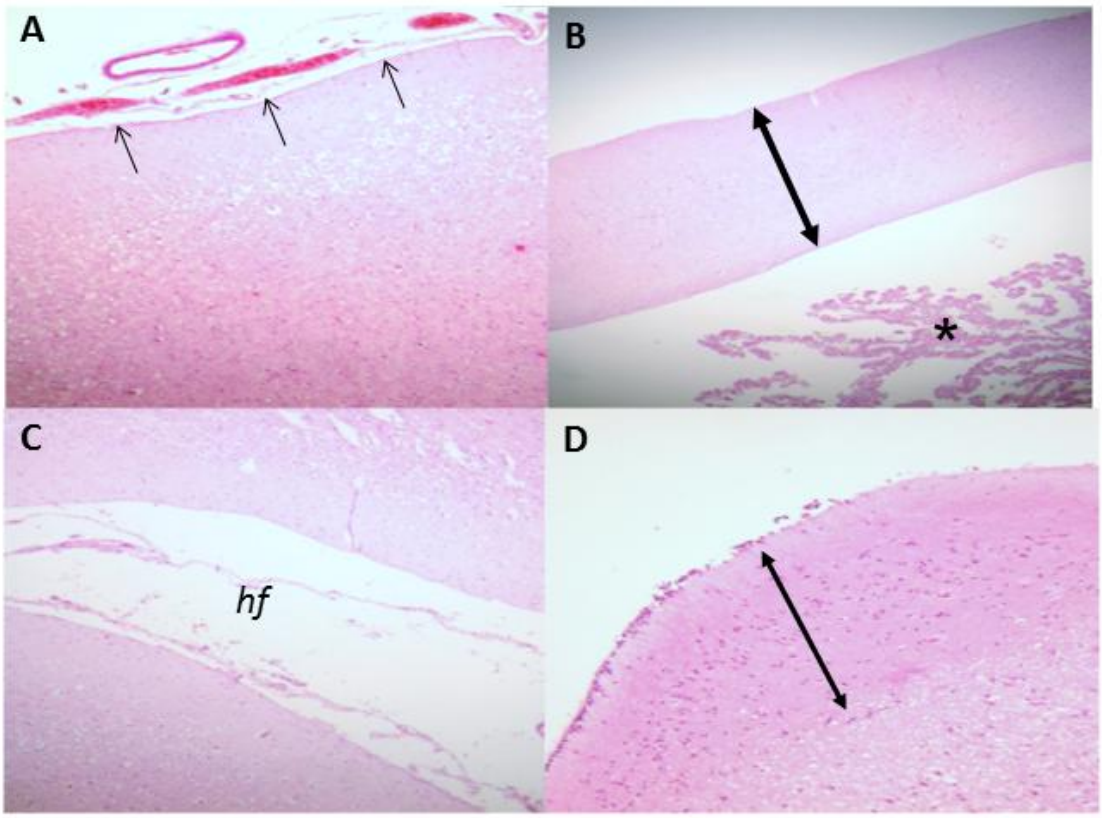

Figure S2. Post Mortem Histopathology of an Affected Child's Cerebral Cortex

Post mortem histology, aged 10 months, A: of parietal cortex from the ascending parietal convolution area, pial surface uppermost. B: taken from the paracentral convolution of the parietal lobe, showing the thinned cortical mantle, expanded lateral ventricle and choroid plexus at the bottom of the figure. C: temporal lobe in the region of the Sylvian fissure, with cortex either side of the horizontal fissure. D: from the mid brain showing the streak like pyramidal tract (slightly darker pink band running upper left to lower right) and is abnormal for a child of this age.

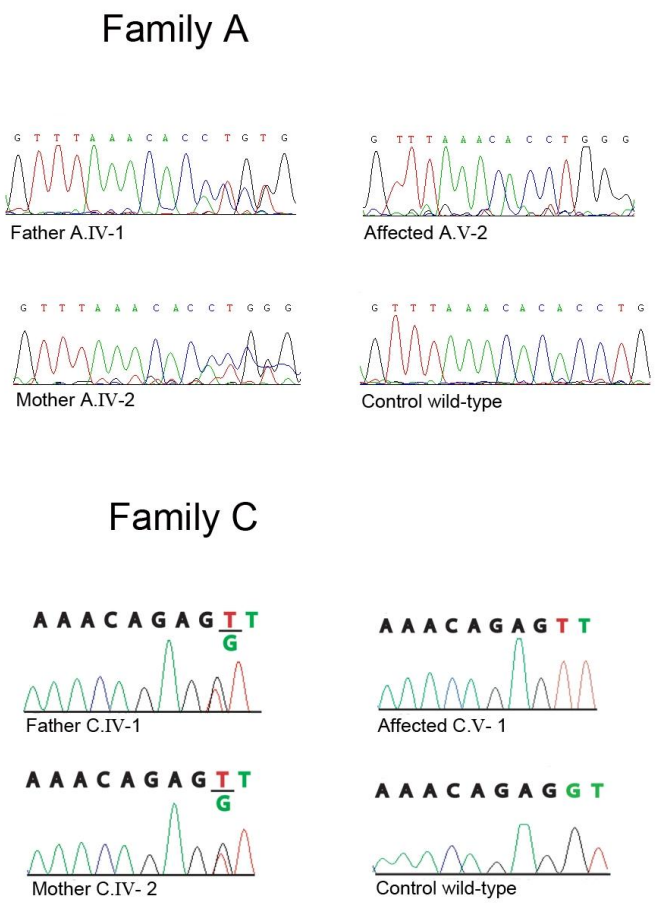

Figure S3. Chromatograms of Genomic *NDE1* for Both Mutations

PCR primers were designed for the genomic sequence of *NDE1* and the genomic DNA was sequenced for the parents and affected siblings in our families. Representative chromatograms are shown for Family A carrying the c.684-685delAC and Family C carrying the c.83+1G>T mutations. The individual identities refers to the familial pedigrees shown in Figure 1.

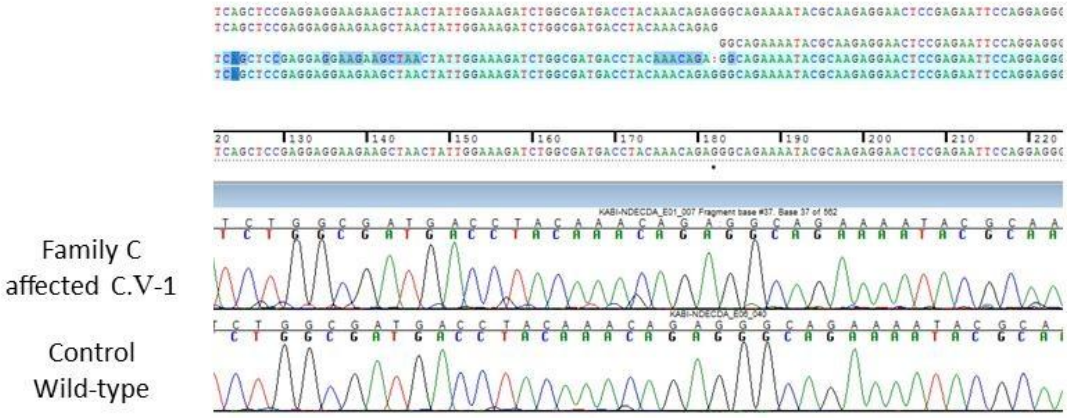

Figure S4. Family C Splice Site Mutation Effect on *NDE1* mRNA

Sequence of mRNA from the affected child (individual C.V-1 in Figure 1) and a control sample. The splice site mutation (c.83+1G>T) creates a cryptic splice site, the wild type sequence being gagGTCAA (exon nucleotides in lower case, intron splice site in capitals). This mutation leads to the last G of the exon now being used as the first G of the splice site; gaGTTCAA. This causes a homozygous loss of G in the mRNA of the affected child (C.V-1) in Family C.

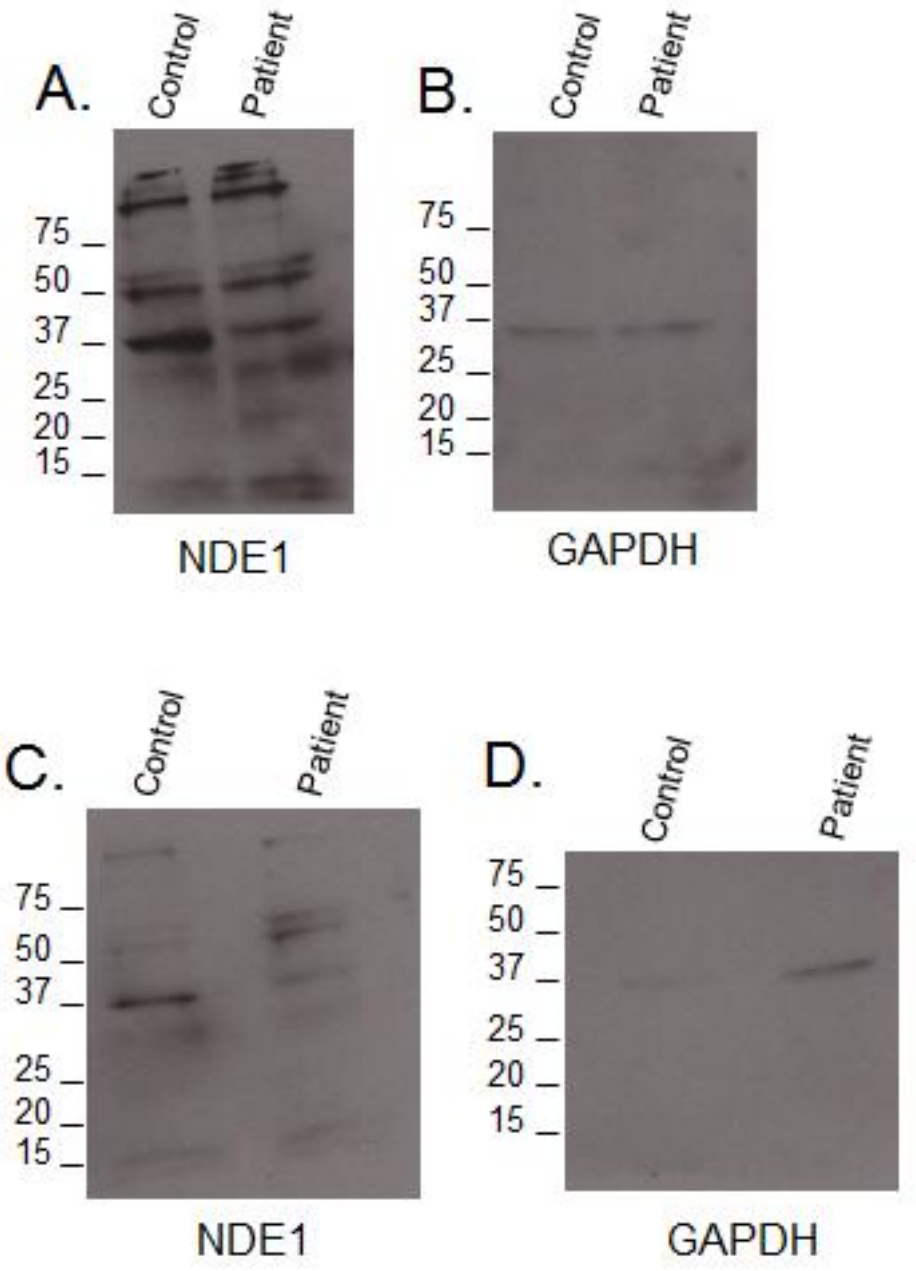

Figure S5. Western Blot Analysis on Protein Lysates Extracted from the Patient's and a Control Subject's Lymphoblastoid Cell Lines

We have performed a Western blot analysis on protein lysates extracted from the patient's (individual C.V-1 in Figure 1) and a control subject's lymphoblastoid cell lines using anti-NDE1 antibody (ProteinTech Group, 10233-1-AP), the epitope of which is not preserved in the mutant peptide. Anti-GAPDH (Santa Cruz Biotechnology, sc-25778) antibody was used as a

loading control. As expected NDE1 was detected in the control as evidenced by a 38kDa band in the blot. Interestingly, a same sized band (38KDa) was also detected in the patient (C.V-1), albeit fainter, with no evidence of an additional band at about 16kDa, which would be indicative of the predicted mutant novel peptide. In the light of the mRNA sequencing from the patient's cell line, which showed the presence of only the mutant RNA, we assume that the NDE1 detection in the patient (C.V-1) can be attributable to the cross-reactivity of the anti-NDE1 antibody with NDEL1, which shares more than 60% identity and 75% similarity with NDE1. Alternatively, a splice isoform excluding the affected exon and thus escaping the effect of the splice site mutation could have been detected in the patient (C.V-1). Indeed, *NDE1* demonstrates alternative splicing and there is evidence of presence of ESTs such as BG760232.1 or BG744425.1 which may account for shorter NDE1 isoforms.

A. NDE1 antibody at a dilution of 1/500, 2 minutes film exposure.
B. Loading control for blot A.; GAPDH antibody at a dilution of 1/200, 1 minute film exposure.
C. NDE1 antibody at a dilution of 1/1000, 2 minutes film exposure.
D. Loading control for blot C.; GAPDH antibody at a dilution of 1/200, 1 minute film exposure.

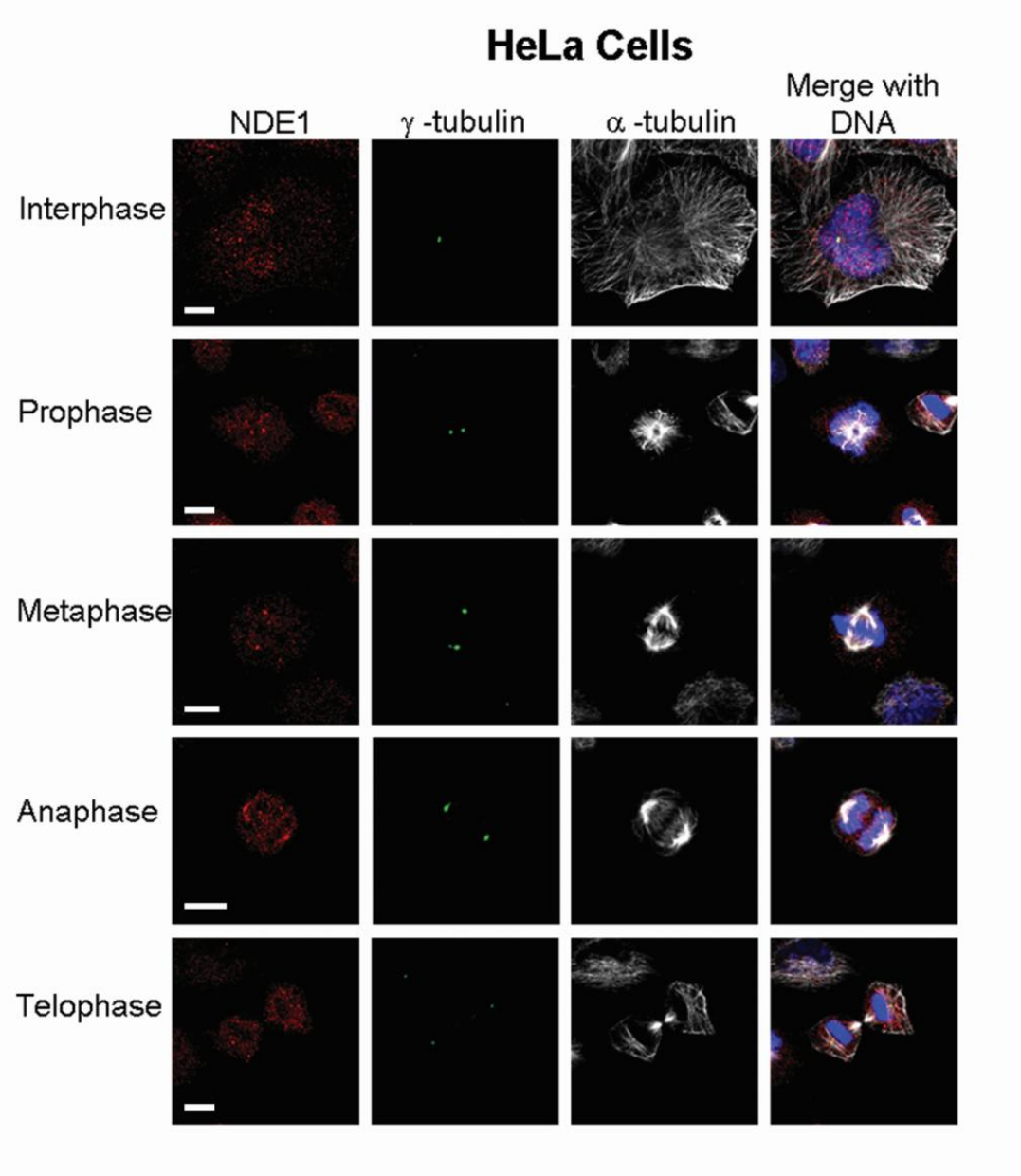
HeLa Cells
NDE1
γ -tubulin
α -tubulin
Merge with DNA
Interphase
Prophase
Metaphase
Anaphase
Telophase

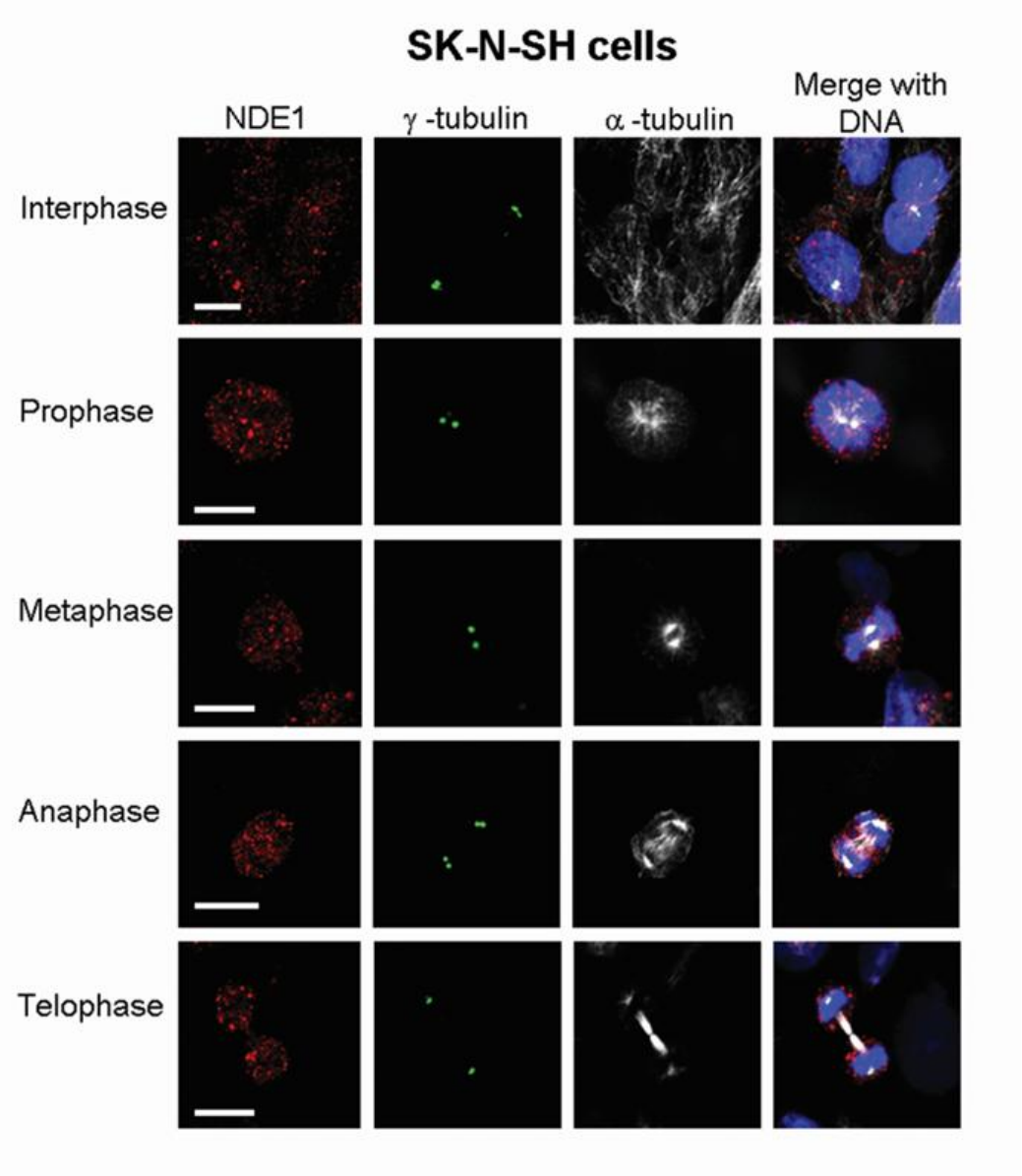

Figure S6. Subcellular Localization of NDE1 throughout the Cell Cycle
Confocal microscopy analysis of HeLa and SK-N-SH cells during each stage of the cell cycle. NDE1 staining is centrosomal throughout mitosis. The intensity of the centrosomal signal goes down in metaphase stage of the cell cycle. In addition to the centrosomal signal, NDE1 also shows some punctate staining in the cytoplasm and nucleus of the cells in both cell lines. Cells were stained with antibodies against human NDE1 (red), γ-tubulin (green) as a centrosome marker, α-tubulin (white) as a microtubule marker, and DNA (blue) stained with DAPI. Scale bar denotes 10 μm.

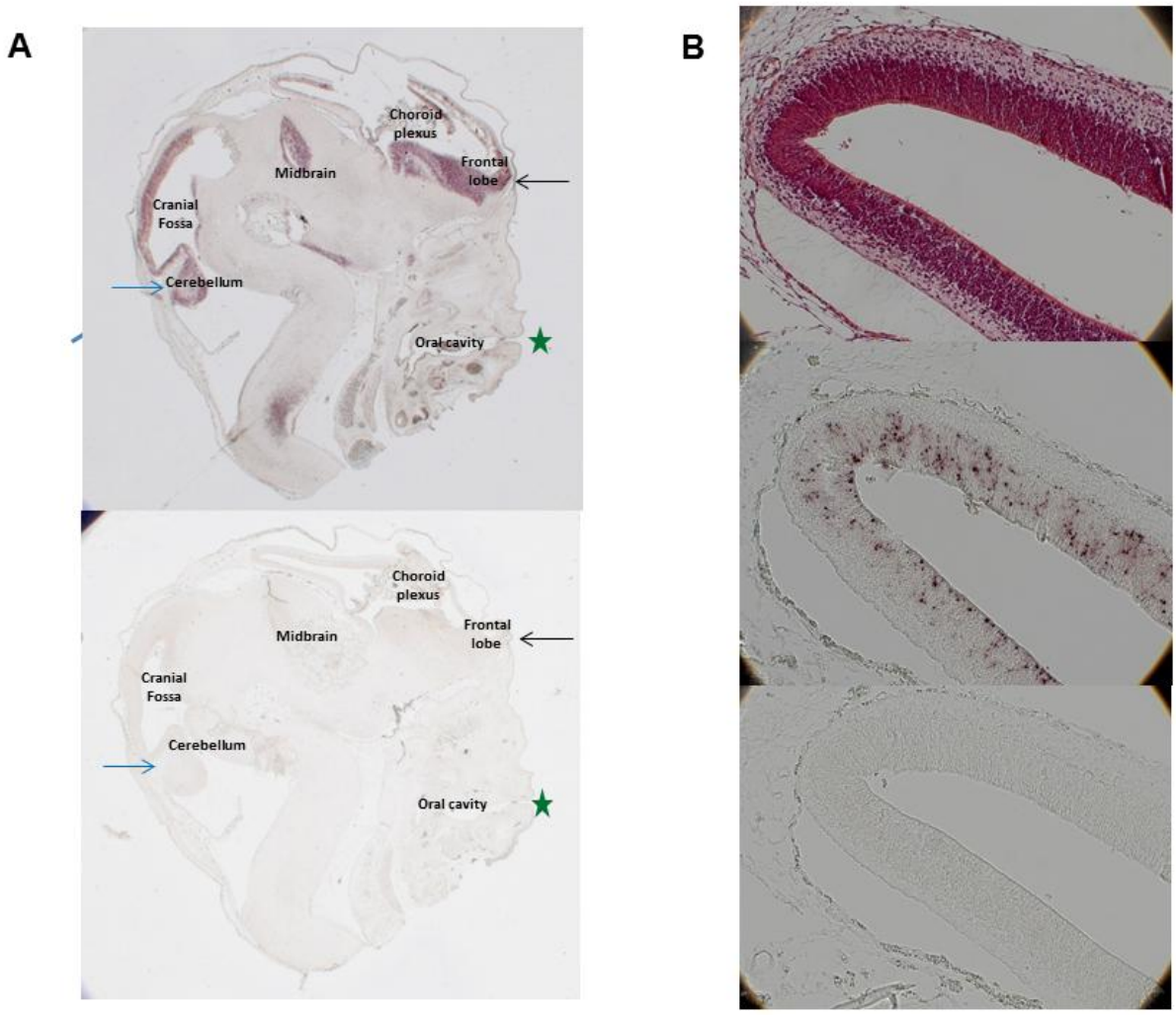

Figure S7. NDE1 Expression in Human CS23 Embryonic Brain

This shows the images from Figure 5A and 5B, and accessory images.

A. *NDE1* expression in a CS23 human embryo head. In situ hybridization using a riboprobe to *NDE1* was performed on a sagittal section of a human embryo. Darker red staining shows expression. The upper image was generated using an antisense riboprobe and shows *NDE1* expression. The lower image was generated using the sense riboprobe, and should be almost blank, and acts as a control. The black arrow shows strong *NDE1* expression in the neuroepithelium of the developing cerebral cortex, and the blue arrow expression in the

neuroepithelium of the developing cerebellum. For orientation of the image the green star shows the mouth, and hence the front of the face.

B. A composite of three consecutively cut 10μm sections through the developing cerebral cortex neuroepithelium. The upper panel is stained with eosin and haematoxylin to show the structure of the neuroepithelium, a dark red colour. The middle panel shows the results of *NDE1* antisense riboprobe in situ hybridization. Only cells within the neuroepithelium are stained. The lower panel shows the results of the sense riboprobe, which acts as a control and should give no significant signal.

Table S1. Homozygosity Intervals for Individual V-1from Family C

Chromosome	Start	End	SNP Start	SNP End	Number of SNPs	Length (cM)	Length (Mb)
2	64,292,394	65,792,102	rs11125993	rs4671683	170	2.51	1.50
4	90,649,718	95,729,661	rs903600	rs4634230	344	2.98	5.08
6	126,089	2,050,976	rs1535053	rs4959632	293	5.89	1.92
9	136,286,902	137,291,321	rs4917339	rs12347149	202	4.48	1.00
12	64,079	1,915,346	rs4980929	rs2429175	214	4.12	1.85
15	23,928,868	37,025,287	rs693798	rs1433876	1,306	27.86	13.10
15	84,251,890	91,405,758	rs8037710	rs3817596	800	14.13	7.15
16	13,787,767	22,732,080	rs4780543	rs2239332	583	13.74	8.94
21	15,498,364	16,699,698	rs2823138	rs6517700	114	2.65	1.20
Total						78.34	41.76

Homozygosity Intervals for the 2 Affected Individuals from Family A

Chromosome	Start (cM)	End (cM)	Number of SNPs	ExcludeR analysis	Length (cM)
3	190.9	203.1	20	significant	12.2
4	52	65.4	60	significant	13.4
12	19.2	29.2	18	significant	10
12	150.7	169.4	25	significant	18.7
16	30.5	51.4	34	significant	20.9

Table S2. Coverage Distributions and Error Rates across the Whole Exome and Homozygosity Intervals

Family ID		C.V-1
Number of lanes		1
Read Type (SR/PE)		SR
Read length		74
Total number of reads (millions)		27.78
% mapped to the genome		97.08
Whole Exome	**% mapped to the exome**	60.01
	Mean coverage	36.2
	% of bases covered at least 4X	94.48
	Mean error rate (%)	0.54
	2nd base error rate (%)	0.13
	Last base error rate (%)	1.53
Exomic Homozygosity Interval	**Exomic interval size (Mbs)**	0.44
	% mapped to the exomic interval	0.85
	Mean coverage	39.58
	% of bases covered at least 4X	92.04
	Mean error rate (%)	0.54
	2nd base error rate (%)	0.13
	Last base error rate (%)	1.5

Table S3. Sensitivity and Specificity for the Detection of Variants

SNP/Sample	C.V-1	
	Sensitivity[+]	**Specificity**
# of Het cSNPs by gt and seq*	2050	
# of called Het cSNPs by seq		2052
# of Het cSNPs by genotyping	2139	
	95.84%	**99.90%**
# of Hom cSNPs by gt and seq	5431	
# of called Hom cSNPs by seq		5485
# of Hom cSNPs by genotyping	5525	
	98.30%	**99.02%**

* Het: heterozygous, cSNP: coding SNP, gt: genotyping, seq: sequencing, Hom: homozygous

[+] Sensitivity=# of cSNPs by gt and seq / # of cSNPs by genotyping

Specificity= # of cSNPs by gt and seq / # of cSNPs by seq

Table S4. Novel Homozygous Variants Identified within the Homozygosity Intervals of Affected Individual 1 of Family C

Chromosome	15	16	16
Position	89,329,010	15,087,045	15,666,220
Base change	G to C	T to C	G to T
Quality score	255	48	78
Coverage	93	7	17
Major allele (no PCR duplicates)	46	7	16
Minor allele (no PCR duplicates)	0	0	0
Gene	PRC1	RRN3	NDE1
Status	Missense	Missense	Splice site
Amino Acid change	H21D	I162V	1 bp downstream of exon 2
Amino Acid position	21/606	162/651	-
PhyloP	2.676	2.366	3.751